Electronic Supplementary Information

High-Performance Water Desalination of Nitrogen- and Sulfur- Codoped Open Hollow Tubular Porous Carbon Electrodes via Capacitive Deionization

Qing Zhang [a], Lingling Hu [a], Dehua Xia [a, b*], Yajing Huang [a], Ping Li [a, b], Li Tan [a], Yongyi Wang [a], Chun He [a, b*], Dong Shu [c], Xi Xie [d]

[a] *School of Environmental Science and Engineering, Sun Yat-sen University, Guangzhou, 510275, China*

[b] *Guangdong Provincial Key Laboratory of Environmental Pollution Control and Remediation Technology, Guangzhou, 510275, China*

[c] *Key Lab of Technology on Electrochemical Energy Storage and Power Generation in Guangdong Universities, School of Chemistry and Environment, South China Normal University, Guangzhou, 510006, China*

[d] *State Key Laboratory of Optoelectronic Materials and Technologies, Sun Yat-Sen University, Guangzhou, 510275, China*

(13 Pages including supplementary 2 Texts and 9 Figures)

[*] Corresponding author: School of Environmental Science and Engineering, Sun Yat-sen University, Guangzhou, 510275, China. Tel.: +86 20 39332690. Email address: xiadehua3@mail.sysu.edu.cn (D.H. Xia); hechun@mail.sysu.edu.cn (C. He).

Text S1. Details on dispersion of MnO_2 nanorods in Experiment processes.

Text S2. Morphology and electrochemical performance of CAC.

Fig. S1 Schematic of capacitive deionization experimental configuration in this work.

Fig. S2 Standard curve of conductivity variation vs. concentration of NaCl solution.

Fig. S3 (a) Digital pictures of hydrogels to synthesize N, S-HTPC (left) and N, S-PC (right); (b) Digital pictures of the dispersed state of MnO_2 nanorods in DI water (left side), β-CD solution (middle) and LB agar@β-CD hydrogel (right side)

Fig. S4 SEM image of HTPC.

Fig. S5 Cyclic voltammograms curves of N, S-HTPC (a), HTPC (b) and N, S-PC (c) electrodes at different scan rates.

Fig. S6 Galvanostatic charge-discharge curves of N, S-HTPC (a), HTPC (b) and N, S-PC (c) electrodes at different current density.

Fig. S7 iR drops of N, S-HTPC, HTPC and N, S-PC electrodes at different current densities.

Fig. S8 SEM image (a), nitrogen adsorption/desorption isotherms (b), pore size distributions (c), cyclic voltammetry curves at 50 mV s^{-1} (d), electrochemical impedance spectra (e) and galvanostatic charge-discharge curves at 0.2 A g^{-1} (f) of CAC sample. (Electrolyte: 1.0 M NaCl aqueous solution)

Fig. S9 CDI profiles of electrosorption capacity variation vs. time (a) and Ragone plots (b) in different initial concentrations of NaCl solution at 1.2 V.

Text S1. Details on dispersion of MnO_2 nanorods in Experiment processes.

The detailed experiment process was as follows: (1) 0.15 g MnO_2 were dispersed in 30 mL DI water by sonication, then placed for 2 h. (left side in **Fig. S3b**) (2) 0.15 g MnO_2 were dispersed in 30 mL β-CD solution by sonication, then placed for 2 h. (middle in **Fig. S3b**) (3) 0.15 g MnO_2 were dispersed in 30 mL mixed solution of β-CD and LB agar by sonication, then placed for 2 h. (right side in **Fig. S3b**) As expected, MnO_2 nanorods easily settled at the bottom of flask due to the gravity, whereas MnO_2 nanorods dispersed well because β-CD functioned as a special surfactant which could make a better dispersed state of MnO_2 nanorods in the presence of β-CD. Furthermore, after the addition of LB agar, LB agar with multitudinous -OH could strongly interact with β-CD to form hydrogel to stabilize the dispersed state of MnO_2 nanorods."

Text S2. Morphology and electrochemical performance of CAC

As shown in **Fig S8a**, the SEM image displayed the rough morphology without open channels of CAC. **Fig. S8b-c** showed that CAC exhibited a high specific surface of 1411 m^2 g^{-1}, close to that of N, S-HTPC, and the pore structure was dominated by micropores. The lack of meso/macropores leads to the insufficient utilization of surface area derived from abundant micropores and the hindrance to ion diffusion, thus resulting in poor capacitive and electrosorption capacities.[1,2] The inferior electrochemical performance of CAC presented by CV, GCD and EIS measurements shown in **Fig. S8d-f** indicated the poor capacitive property due to the lack of meso/macropores structure."

References

1. C. L. Yeh, H. C. Hsi, K. C. Li and C. H. Hou, Improved performance in capacitive deionization of activated carbon electrodes with a tunable mesopore and micropore ratio, *Desalination*, 2015, **367**, 60-68.
2. T. Alencherry, A. R. Naveen, S. Ghosh, J. Daniel and R. Venkataraghavan, Effect of increasing electrical conductivity and hydrophilicity on the electrosorption capacity of activated carbon electrodes for capacitive deionization, *Desalination*, 2017, **415**, 14-19.

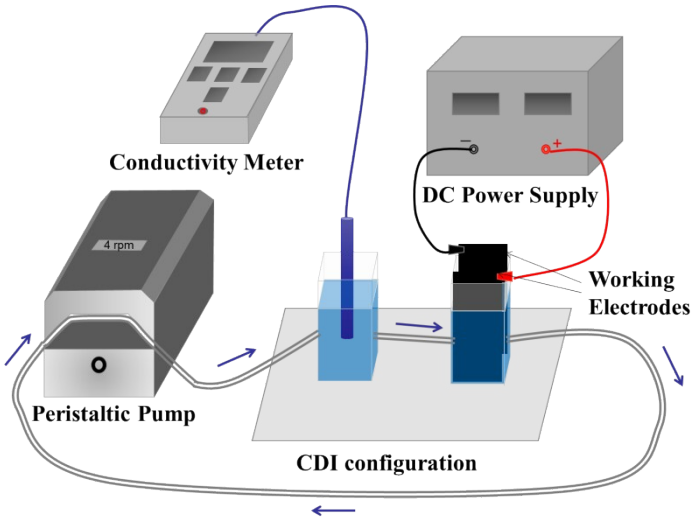

Fig. S1 Schematic of capacitive deionization experimental configuration in this work.

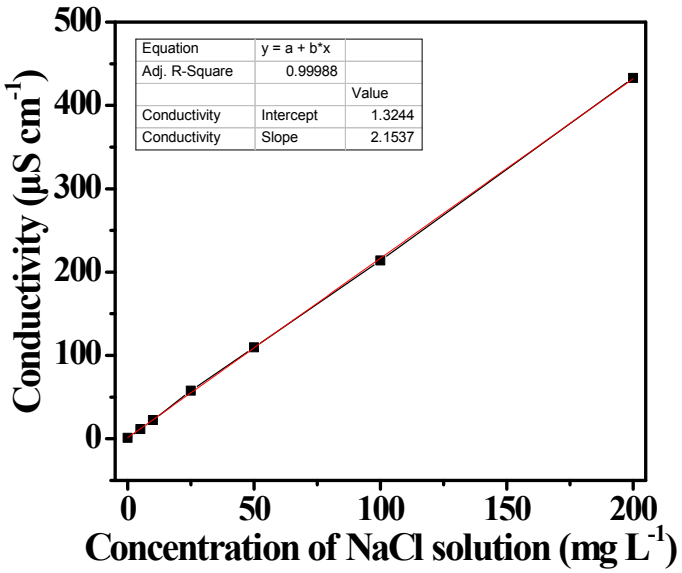

Fig. S2 Standard curve of conductivity variation vs. concentration of NaCl solution.

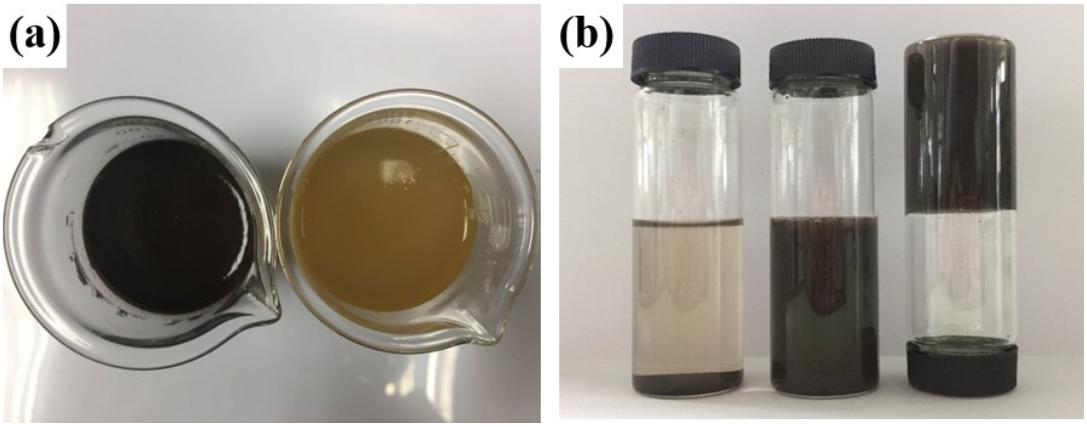

Fig. S3 (a) Digital pictures of hydrogels to synthesize N, S-HTPC (left) and N, S-PC (right); (b) Digital pictures of the dispersed state of MnO_2 nanorods in DI water (left side), β-CD solution (middle) and LB agar@β-CD hydrogel (right side)

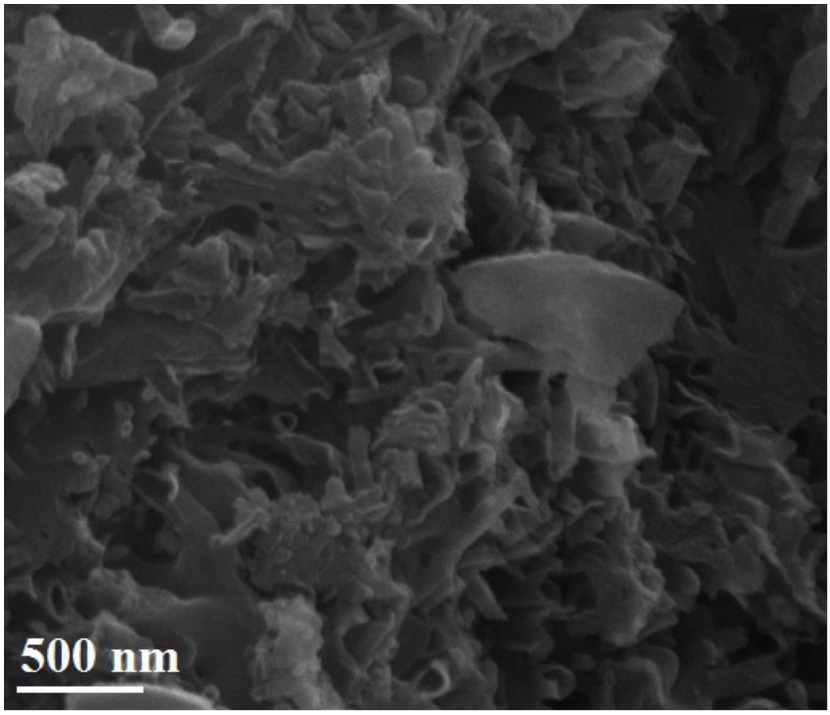

Fig. S4 SEM image of HTPC.

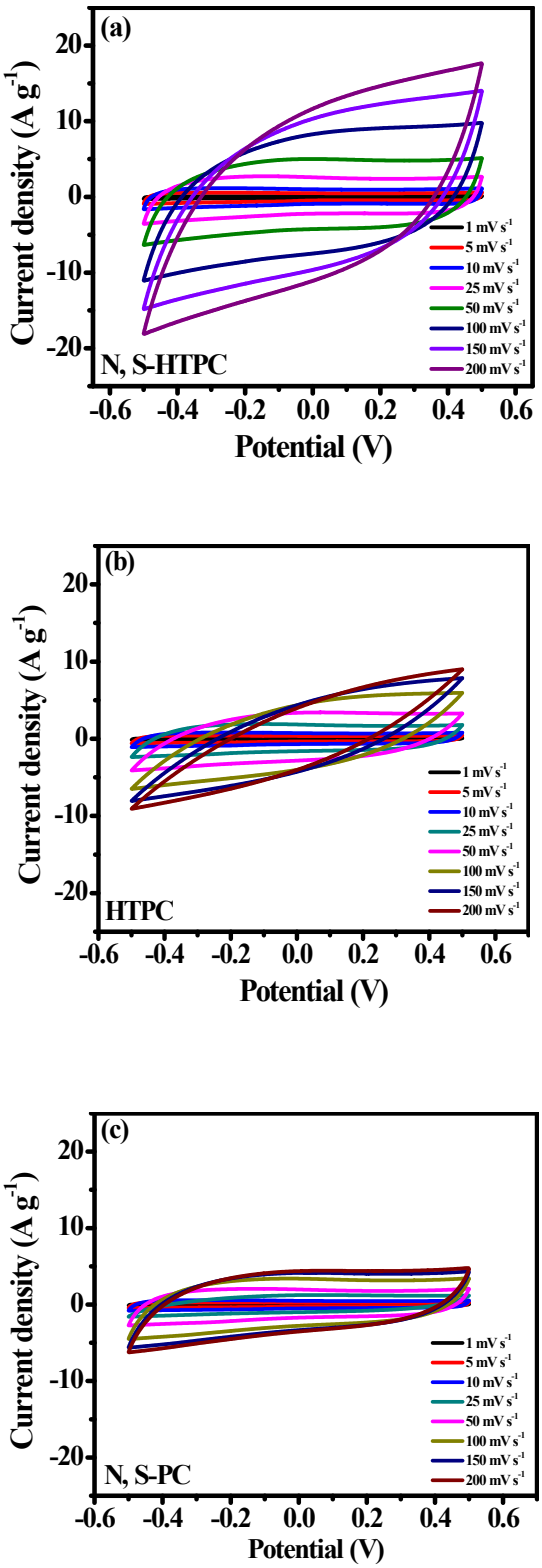

Fig. S5 Cyclic voltammograms curves of N, S-HTPC (a), HTPC (b) and N, S-PC (c) electrodes at different scan rates.

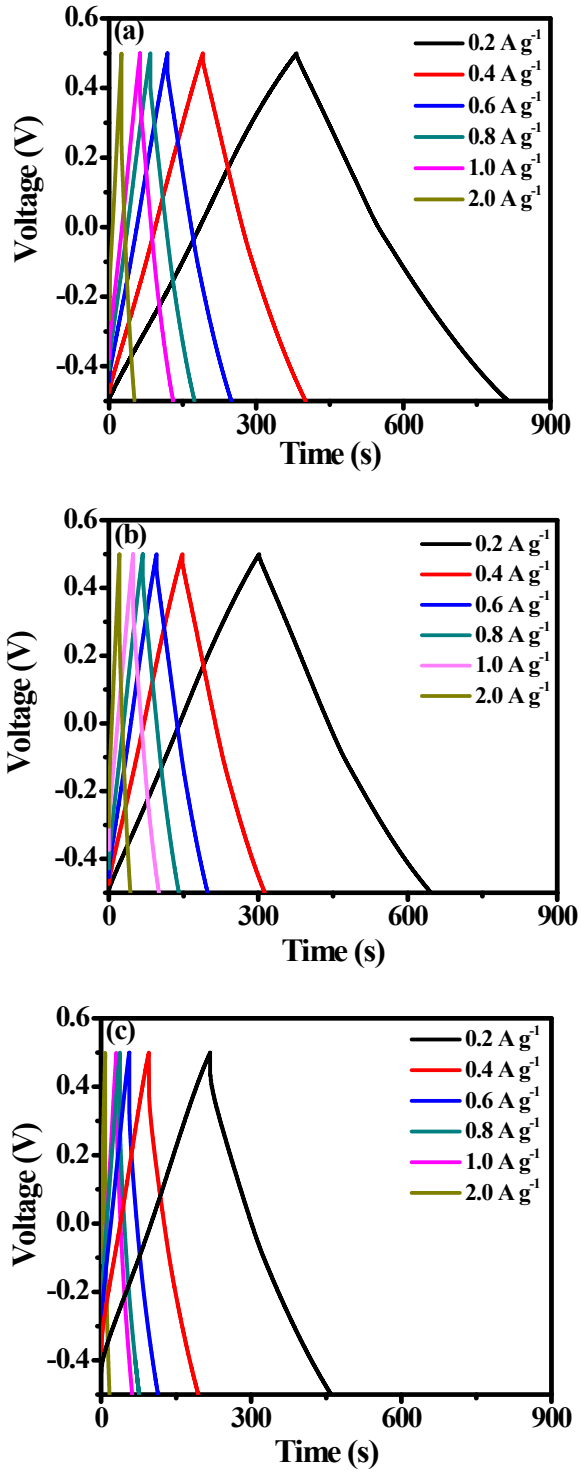

Fig. S6 Galvanostatic charge-discharge curves of N, S-HTPC (a), HTPC (b) and N, S-PC (c) electrodes at different current densities.

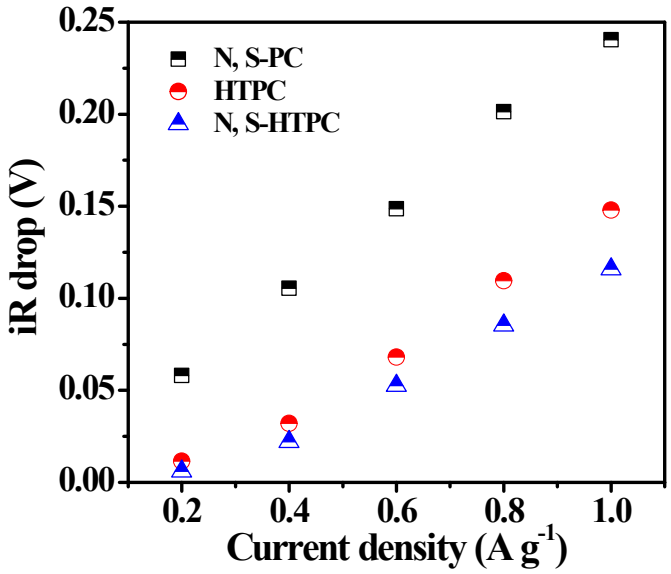

Fig. S7 iR drops of N, S-HTPC, HTPC and N, S-PC electrodes at different current density.

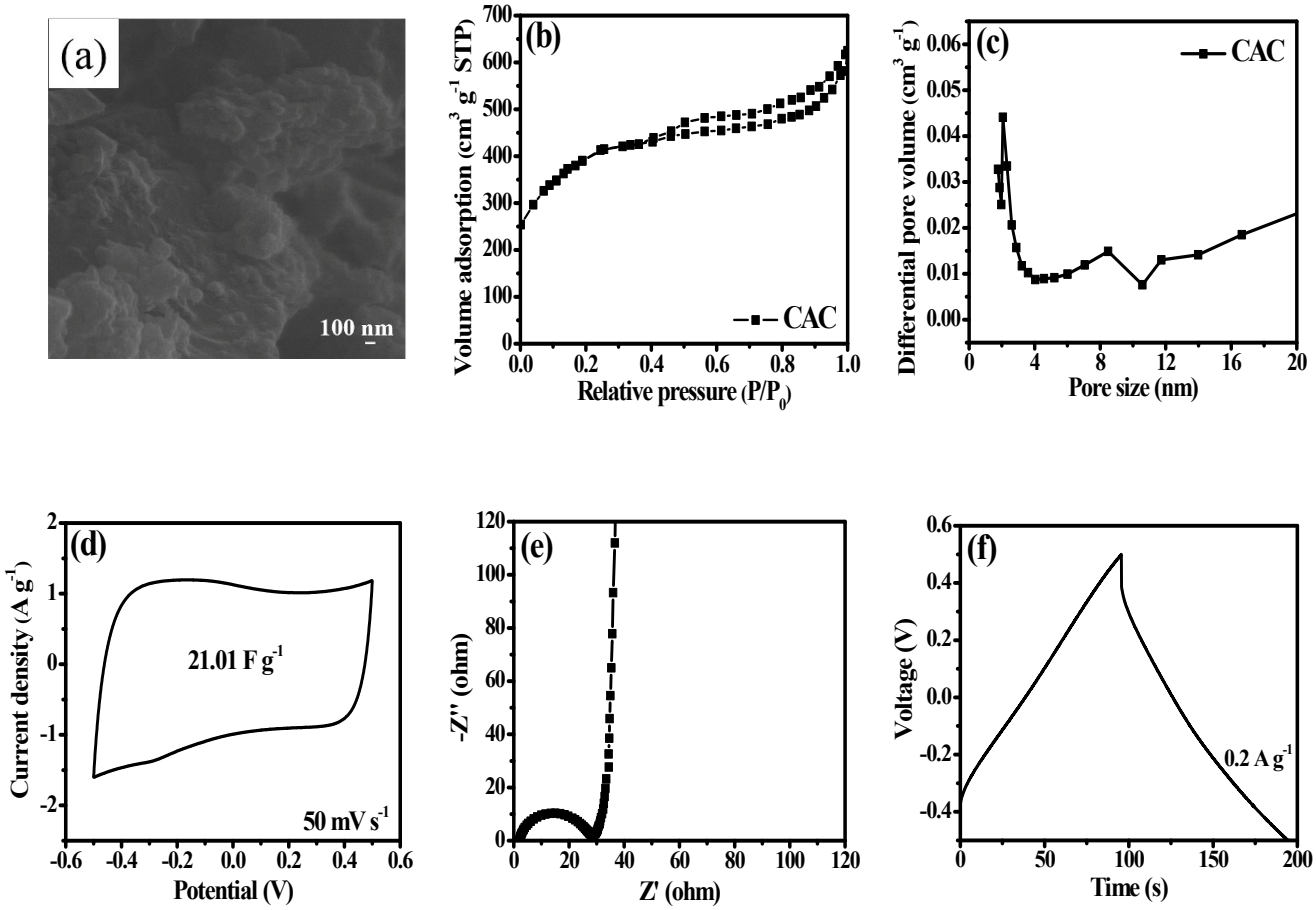

Fig. S8 SEM image (a), nitrogen adsorption/desorption isotherms (b), pore size distributions (c), cyclic voltammetry curves at 50 mV s^{-1} (d), electrochemical impedance spectra (e) and galvanostatic charge-discharge curves at 0.2 A g^{-1} (f) of CAC sample. (Electrolyte: 1.0 M NaCl aqueous solution)

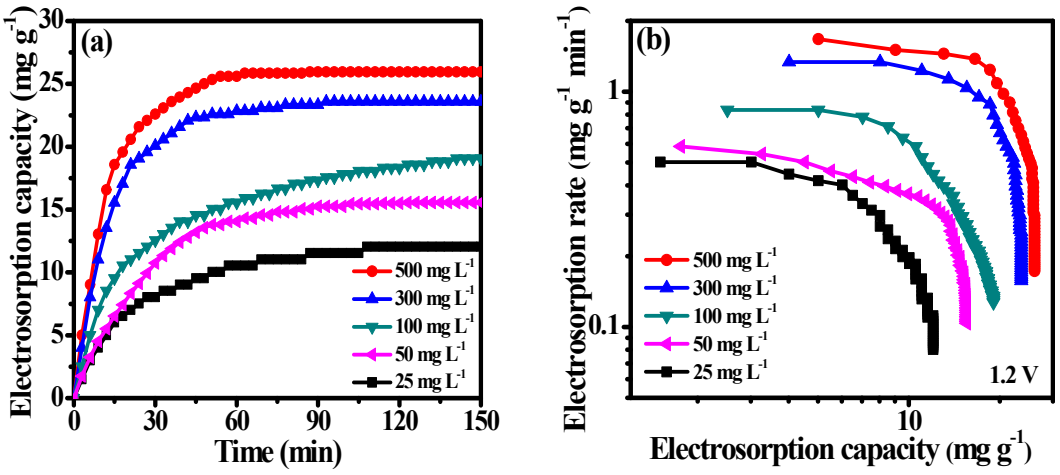

Fig. S9 CDI profiles of electrosorption capacity variation vs. time (a) and Ragone plots (b) in different initial concentrations of NaCl solution at 1.2 V.